engineering proceedings

MDPI

Proceeding Paper

Rare-Earth Ion-Doped Zinc Oxide as a Viable Photoanode Material for Dye-Sensitized Solar Cells: Optoelectrical and Wettability Aspects †

Altamash Shabbir [1,*], Zuhair S. Khan [2,*], Hina Pervaiz [1] and Hafiz Muhammad Haseeb [1]

[1] U.S—Pakistan Centre for Advanced Studies in Energy, National University of Sciences and Technology, Islamabad 44000, Pakistan; hpervaizphdf19.ces@student.nust.edu.pk (H.P.); haseebwahla519@gmail.com (H.M.H.)
[2] Research Innovation and Commercialization (ORIC) Directorate, University of Wah, Wah Cantt 47040, Pakistan
* Correspondence: altamashnust19@gmail.com (A.S.); dr.zskhan786@gmail.com (Z.S.K.)
† Presented at the 8th International Electrical Engineering Conference, Karachi, Pakistan, 25–26 August 2023.

Abstract: In the realm of renewable energy harvesting, nanomaterials doping with rare-earth ions is gaining traction. Lanthanum-doped ZnO thin films were synthesized using the sol–gel technique, with various La weight percentages. The X-ray diffraction (XRD) findings indicated that the hexagonal wurtzite structure of lanthanum-doped ZnO was maintained at various La weight percentage, despite a variation in the average crystallite size from 39 nm to 26 nm. The granule-like structure was examined using scanning electron microscopy (SEM), and the morphology remained unchanged with the inclusion of lanthanum. The direct energy bandgap was estimated to extend from 3.55 eV to 3.40 eV, revealing a discernible shift as the lanthanum concentration increased. The dc electrical conductivity of the films improved as the lanthanum doping in the ZnO lattice structure increased. Furthermore, increasing the La content altered the water contact angles from 51.5° to 26.4°, making the surface more hydrophilic. These findings can allow for the ubiquitous development of nanostructures for photoanode materials made of metal oxides with future applications in DSSC devices.

Keywords: dye-sensitized solar cell; lanthanum doped ZnO; photoanode; optoelectrical properties; hydrophilic

Citation: Shabbir, A.; Khan, Z.S.; Pervaiz, H.; Haseeb, H.M. Rare-Earth Ion-Doped Zinc Oxide as a Viable Photoanode Material for Dye-Sensitized Solar Cells: Optoelectrical and Wettability Aspects. *Eng. Proc.* **2023**, *46*, 19. https://doi.org/10.3390/engproc2023046019

Academic Editors: Abdul Ghani Abro and Saad Ahmed Qazi

Published: 21 September 2023

1. Introduction

Renewable energy is advantageous because it helps reduce greenhouse gas and air pollution emissions [1,2]. The photovoltaic technology directly converts sunlight into electricity without using any mechanical components. The first-generation photovoltaic solar cells, known as conventional cells, consist of single-crystal silicon wafers. The second generation is based on polycrystalline silicon and involves the application of amorphous thin-film methods. The third generation of PVSCs is currently in development and includes perovskite, polymer hetero-junctions, and DSSC thin-film technologies [3]. The DSSC technology has gained attention due to its affordability, simplicity, and high photo-to-electric conversion efficiency. However, there are still significant challenges to be faced to enhance their efficiency. DSSCs consist of a photoanode, a sensitizer, a counter electrode, and a redox-coupled electrolyte, with the photoanode being the most important component. The photoanode performs critical functions such as dye loading, electron collection, and electron transportation. A high-performance solar cell requires a photoanode with desirable qualities, including a significant surface area, a smooth surface morphology, and minimal grain boundaries to allow a fast electron transportation [4].

The photoanodes used in solar cells are typically made of metal oxide semiconductors with a wide bandgap (>3 eV), such as titanium dioxide, zinc oxide, tin oxide, and niobium

oxide. These materials are preferred because they possess desirable electrical properties and are resistant to photocorrosion [5,6]. The performance of semiconductors may be hampered by photo corrosion, which occurs when holes (produced during bandgap stimulation) are oxidized by redox electrolytes. The best photoanode material in DSSCs nowadays is represented by TiO_2 nanoparticle because of its excellent efficiency. TiO_2 also has the advantages of being inexpensive, easily accessible, non-toxic, and biocompatible. Due to its broad bandgap semiconducting properties, however, TiO_2 presents no visible-light absorption [6]. ZnO is being considered as a potential candidate for use in photoanodes for DSSCs. This is due to its favorable characteristics such its appropriate direct bandgap and a conduction band that is comparable to that of TiO_2. Furthermore, ZnO offers two significant advantages over TiO_2: ZnO has substantially better electrical mobility, less charge recombination, and its nanostructures' shape are simple to modify. ZnO structure was designed using VESTA software (version 3) and is shown in Figure 1.

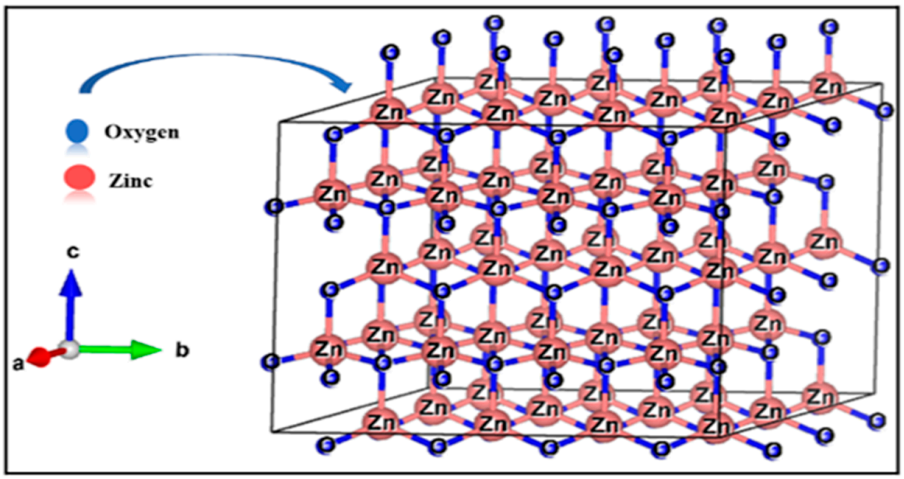

Figure 1. ZnO structure simulated using VESTA software (version 3).

Rare-earth ions, such as lanthanum (La), can be used as dopants in zinc oxide (ZnO) for dye-sensitized solar cells (DSSCs) because they have unique optical and electronic properties that can enhance the performance of DSSCs [7]. One important property is their ability to increase the absorption of light in the visible and near-infrared regions of the electromagnetic spectrum. This is because rare-earth ions present f-shell electronic transitions that are relatively narrow and well-defined, which can lead to sharp absorption peaks in this spectral range. By doping ZnO with rare-earth ions, the absorption of light in the visible and near-infrared regions can be increased, which improves the efficiency of DSSCs. In addition, rare-earth ions can also improve the charge transport properties in DSSCs by reducing the recombination of electrons and holes at the semiconductor–electrolyte interface. This can result in DSSCs with higher efficiency and stability [8]. In this research, a wet chemistry method was applied to produce thin films of ZnO that were either pure or doped with La at various weight concentrations. The produced thin films were then analyzed using different characterization techniques to determine their crystalline structure, a s well as their morphological, functional group, optoelectrical, and wettability features. These techniques included XRD, SEM/EDS, FTIR, UV–Vis, Hall Effect, and water contact angle measurements.

2. Experimental Setup

To produce zinc oxide films, the sol–gel method was employed, and different amounts of lanthanum were added (0%, 2.5%, and 5%, wt. %). The primary materials were zinc acetate dehydrate and lanthanum nitrate hexahydrate. The glass substrates used were either ordinary glass or conducting glass FTO, both with a size of 2×2 cm^2 and a thickness

of 2.2 mm. Ethanolamine, absolute methanol, and absolute ethanol with a purity level of 99.9% were utilized; they were obtained from Sigma-Aldrich (St. Louis, MO, USA).

A coating solution was produced by dissolving zinc acetate dihydrate and lanthanum nitrate hexahydrate in anhydrous ethanol and methanol. An equimolar amount of the sol stabilizer monoethanolamide (MEA) was added to the solution. The solution contained a total concentration of 0.5 mol/L of Zn^{2+} and La^{3+} ions. The solution was stirred and refluxed at 70 °C for 3 h, obtaining a clear and uniform solution. After aging the solution for 24 h, it was spin-coated onto the substrate at 2500 rpm for 30 s. The films were preheated at 180 °C for 5 min, to remove volatile compounds from the substrate surface. To obtain a thickness of 700–800 nm, the thin film deposition process was performed six times. The films were then subjected to annealing at 450 °C in air for one hour to promote crystallization. This process was undertaken to modify the films' physical and chemical properties for use in a range of applications, such as electronic devices, sensors, or optical coatings.

Numerous analytical techniques were employed to examine the ZnO thin films: PXRD to determine their purity and crystalline structure, SEM to examine the surface morphology, FTIR and UV–Vis spectrometry to determine the structural, functional, and optical properties, Hall Effect measurements to evaluate the electrical properties, and tensiometer to measure the water contact angle and assess the wettability and dye adsorption potential in solar applications.

3. Results and Discussion

3.1. Phase Analysis

The crystal structure of undoped and La-doped ZnO thin films was examined using XRD. Both types of films presented clear peaks in the 20–70-degree range, as shown in Figure 2, indicating that they were crystalline after annealing at 450 °C. The peaks were identified as corresponding to the (100), (002), (101), (110), (103), and (112) planes of ZnO, according to the JCPDS Card No. 36-1451. The XRD pattern showed that La-doping did not introduce any secondary phases and resulted in a hexagonal wurtzite phase. The (002) peak in the La-doped film shifted to higher angles, suggesting the successful integration of rare-earth ions into the ZnO lattice. The intensity of the peak decreased as the concentration of lanthanum increased up to 5 wt. %, which could be due to the influence of lanthanum on ZnO nucleation. The crystallite size was determined using the FWHM of the XRD peaks and the Scherer formula, reported in Equation (1):

$$D_s = \frac{0.9\lambda}{B\cos\theta} \quad (1)$$

where *Ds*, λ, *k*, θ, and β are symbols used in X-ray diffraction analysis to represent the size of a crystallite, the wavelength of the X-ray, the shape factor, the Bragg diffraction angle, and the FWHM, respectively [9]. In the XRD pattern depicted in Figure 2, the (002) characteristic peak of the La-doped ZnO thin film shifted to a higher angle (34.42°) compared to the peak of the undoped ZnO film (34.35°). This shift can be attributed to the successful incorporation of the lanthanum ions into the ZnO lattice, leading to a strain or a distortion of the lattice. The insertion of La^{3+} ions into the ZnO lattice might cause lattice expansion, which would increase the distance between the (002) lattice planes and cause the peak to shift towards higher angles. Therefore, the peak shift in the XRD pattern indicated that the lanthanum ions were effectively introduced into the ZnO crystal structure, altering its lattice parameters. The introduction of rare-earth metal dopants caused a decrease in the typical crystallite sizes from 39 nm to 26 nm, as determined by the Scherrer formula. This was also observed by Anandan et al., who suggested that the suppression was directly linked to the distortion of the crystal lattice resulting from the larger ionic radius of the lanthanum cation (1.15 Å) compared to the zinc cation (0.74 Å) [10].

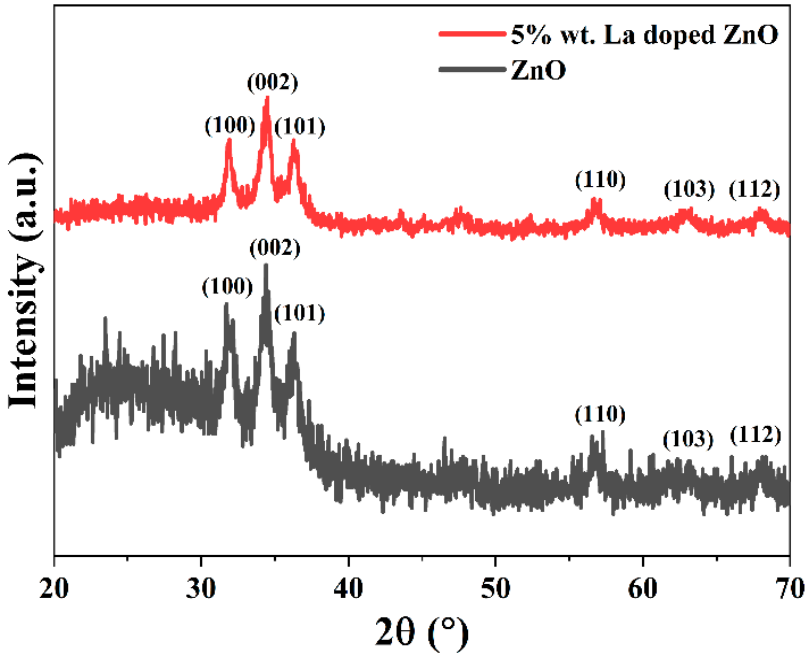

Figure 2. XRD diffractograms of bare and 5 wt. % La-doped ZnO.

3.2. Morphological Analysis

SEM analysis was used to examine the surface morphology, particle size, and growth rate of the synthesized samples. The films exhibited a granular structure with closely packed grains as depicted in Figure 3a,b. By using Image J software (https://imagej.net/ij/), the particle size distribution of the granules was determined as shown in Figure 3c,d, and it was found that the particle size decreased from 54 nm to 36 nm as lanthanum doping increased up to 5 wt. %, consistent with the XRD analysis. This study investigated the effects of La doping in ZnO for photoanode materials. La addition did not extensively alter the morphology of the pure ZnO thin film, suggesting a little impact on the growth mechanism and crystal structure, which was confirmed by the XRD analysis. The chemical analysis confirmed the purity of the films and the successful incorporation of La without additional impurities.

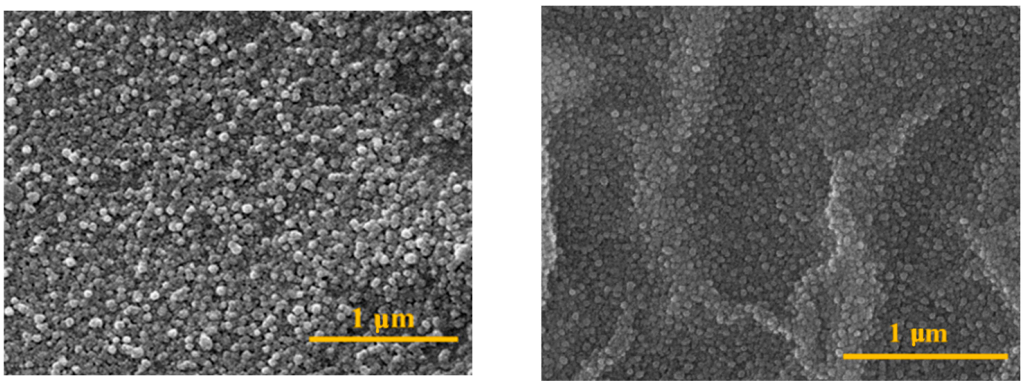

(**a**) (**b**)

Figure 3. *Cont.*

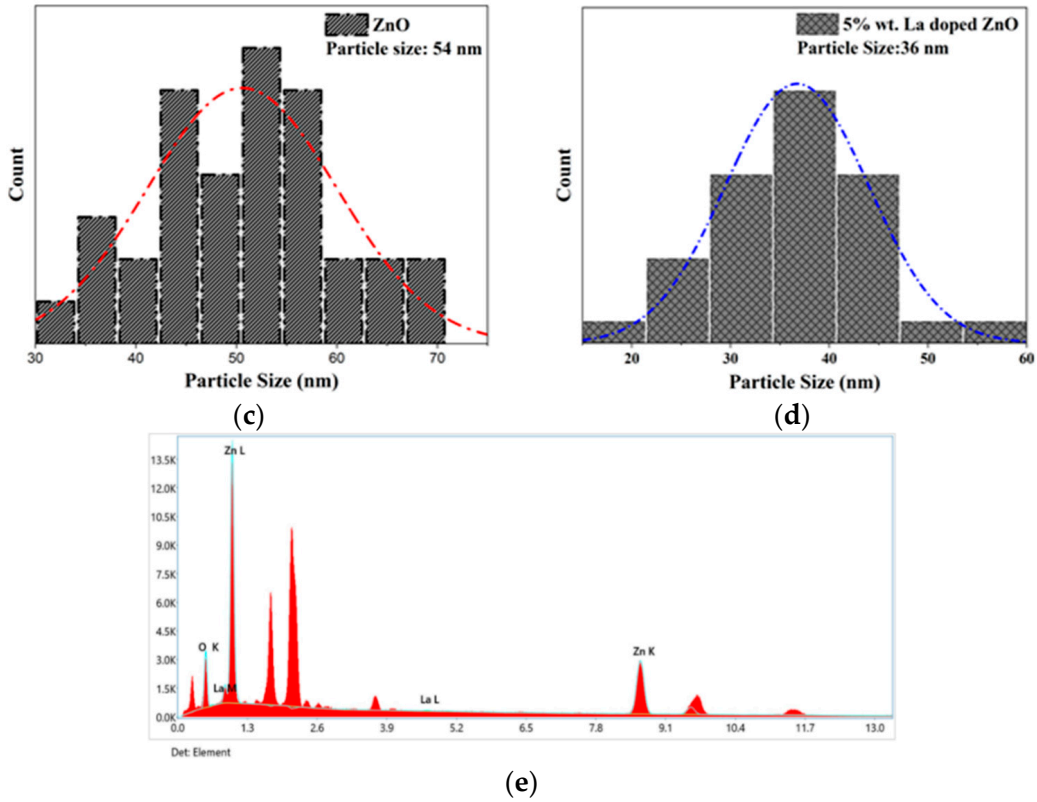

Figure 3. (**a**–**e**). Scanning electron microscopic images. (**a**) Bare ZnO, (**b**) 5 wt. % La-doped ZnO, (**c**) particle size distribution curve of ZnO, (**d**) particle size distribution curve of La doped ZnO, (**e**) energy-dispersive X-ray (EDX) spectra of 5 wt. % La-doped ZnO.

3.3. Structural Inspection

FTIR analyses use infrared radiation to identify the functional groups and structural characteristics of a material. In this case, the La-doped ZnO thin films were studied using FTIR analysis after being annealed at 450 °C, as shown in Figure 4. The analysis provided information about the types of chemical bonds and the structural properties of the films, which can be useful for understanding their properties and potential applications. Due to the presence of stabilizers, ethanol, and methanol, the doped ZnO thin film exhibited small intense peaks corresponding to C-C, C=C, and hydrogenated carbon at 1300–2360 cm^{-1} [11,12]. The peaks at 591 cm^{-1} and 687–756 cm^{-1} indicated a stretching vibration of zinc and oxygen associated with the oxygen sublattice (E_{2H}) vibration, oxygen vacancies, and the successful integration of lanthanum into the ZnO lattice structure, respectively [13]. These peaks were caused by the deformation of the vibrational mode. The solvents adsorbed in the Zinc oxide structure determined a wide adsorption band corresponding to the hydroxyl group (-OH) in the 3200–3700 cm^{-1} region, as shown in Figure 4 [11]. FTIR subsequently measured the Zn-O vibrational mode with a wurtzite hexagonal structure, which revealed the presence of lanthanum in the zinc oxide lattice structure.

3.4. UV–Vis Spectrophotometry

As depicted in Figure 5, both the pure and the La-doped ZnO exhibited strong absorption in the UV range, specifically in the 300–400 nm range. The band-edge absorption of the synthesized materials was found in the near-UV region, approximately at 348–365 nm. The addition of lanthanum to the ZnO lattice caused a significant reduction in the energy bandgap (E_g), which decreased from 3.55 to 3.40 eV as the doping concentration increased

from 0 to 5 wt. %. The E_g for the direct transition was calculated using Equation (2), plotting $(hv)^2$ versus hv and extrapolating its linear portion to ($hv^2 = 0$) [14]:

$$\alpha = \left(\frac{A}{hv}\right)[hv - E_g]^m \quad (2)$$

where α is the absorption coefficient, h is the Planck's constant, v is the frequency, and E_g is the optical bandgap. The reduction in the bandgap of ZnO doped with 5 wt. % of La can be explained by the incorporation of La^{3+} ions into the ZnO lattice. Photoanode materials such as ZnO doped with La^{3+} ions exhibit lattice defects due to the larger ionic radius of La^{3+} compared to Zn^{2+} ions. These defects introduce new energy levels within the bandgap, acting as traps for electrons and holes. As a result, impurity levels form, reducing the bandgap energy [15]. The overlap between impurity levels and the valence or conduction bands enhances the photoelectrochemical properties, increasing the probability of electron–hole pair generation and making these materials suitable candidates for the production of efficient photoanodes for various applications.

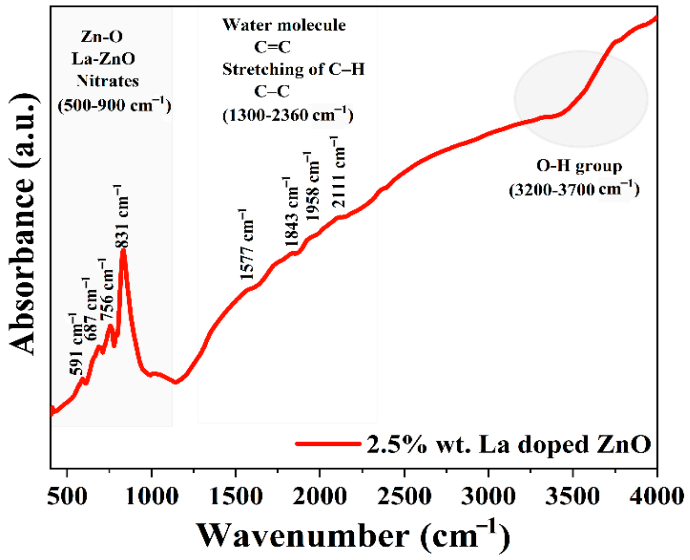

Figure 4. FTIR spectra of the 2.5 wt. % La-doped ZnO film.

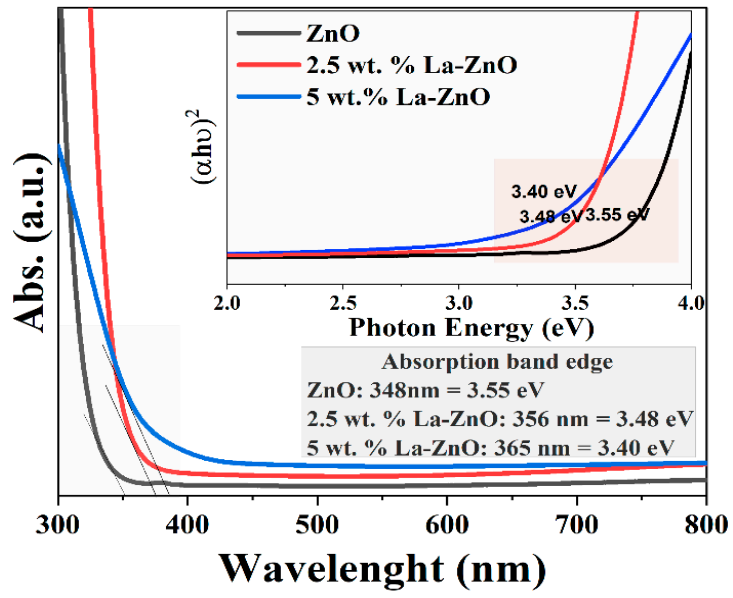

Figure 5. Absorption spectra of pure and doped ZnO; insert: spectra of the direct band.

3.5. Hall Effect Measurement

The Hall Effect measurement is used to determine the electrical properties of materials. The conductivity of the ZnO lattice improved, and its resistivity decreased after doping with La because La doping introduced free carriers in the material. The La^{3+} cations replaced the Zn^{2+} cations in the ZnO lattice, generating oxygen vacancies and free electrons. These free electrons acted as charge carriers in the material, leading to an increase in electrical conductivity. The introduction of La^{3+} ions through Zn^{2+} ion substitution led to an increased concentration of charge carriers within the material, consequently improving its electrical conductivity. The electrical resistance of the thin films decreased with increasing lanthanum concentrations, and the minimum resistance of 3.36×10^{1} Ω.cm was obtained for a film with a 5 wt. % lanthanum content as shown in Table 1. The conductivity of the 5% lanthanum-doped ZnO was 1.55×10^{-2} S/cm, i.e., within the conductivity range of semiconductors. The carrier concentration for pure ZnO was 2.4×10^{13}, while it was 3.2×10^{15} for 5 wt. % lanthanum-doped ZnO. This increase in carrier concentration indicated an increase in bulk concentration and charge mobility. The rise in carrier concentration and conductivity in lanthanum-doped ZnO was due to the interaction between electrons and impurities, as well as by the Coulomb interaction between carriers [16]. Generally, the doping of La of a ZnO lattice structure introduces free carriers in the material, leading to an increase in electrical conductivity and mobility of the charge carriers. These leads to a decrease in the electrical resistivity and an increase in carrier concentration compared to pure ZnO. The values obtained for electrical resistance, conductivity, and carrier concentration in this study suggest that La-doped ZnO can be used in photoanodes and transparent conductive layers that require good electrical conductivity.

Table 1. Illustration of the electrical response for bare and doped ZnO specimens.

Sample ID	Electrical Parameters			Type
	ρ (10^{1} Ω.cm)	σ (10^{-2} 1/Ω.cm)	n_H (cm^{-3})	
Pure ZnO	24.7	0.32	2.4×10^{13}	n-type
2.5 wt. % LZO	16.5	0.89	7.3×10^{14}	n-type
5 wt. % LZO	3.36	1.55	3.2×10^{15}	n-type

Note: ρ, resistivity, σ, conductivity, nH, bulk concentration.

3.6. Water Contact Angle (WCA) Measurement

A surface's wetting properties are highly significant for a range of reasons, both practical and scientific. To determine a surface's adhesion and free energy properties, it is necessary to evaluate both its roughness and its composition [17]. A surface is considered hydrophilic if a water droplet can wet it and form an angle between 0° and 90°, while as it is deemed hydrophobic if the liquid cannot wet it and forms an angle between 90° and 180°. Equation (3) is commonly used to calculate the WCA, which depends on both the surface free energy of the material and the work of adhesion between the liquid and the solid surface:

$$\cos\theta = (\gamma_{SV} - \gamma_{Sl})/\gamma_{lV} \quad (3)$$

The symbols γ_{sv}, γ_{sl}, and γ_{lv} represent the surface tensions between the solid and the vapor phases, the solid and the liquid phases, and the liquid and the vapor phases, respectively [18].

The water contact angle (WCA) of pure ZnO was found to be 51.5°, while after doping with La, it decreased to 26.4°, as shown in Figure 6. This change in the WCA could be attributed to various factors such as alterations in the microstructure and residual stresses resulting from doping [19]. La doping caused the formation of a hydrophilic surface on the material with high surface energy. The alignment of ZnO thin films along a particular axis was significantly reduced after doping with 5.0 wt. % of La. The surface free energy densities were 9.9, 12.3, and 20.9 eV/nm^2 for the (002), (110), and (100) planes,

respectively [20]. The decrease in the WCA values could be due to an increase in the material's surface free energy as the doping level increased, as the preferred orientation along a particular axis was significantly suppressed after doping with La. Therefore, this finding indicated that a material's hydrophilic property can enhance dye adsorption within the photoanode material.

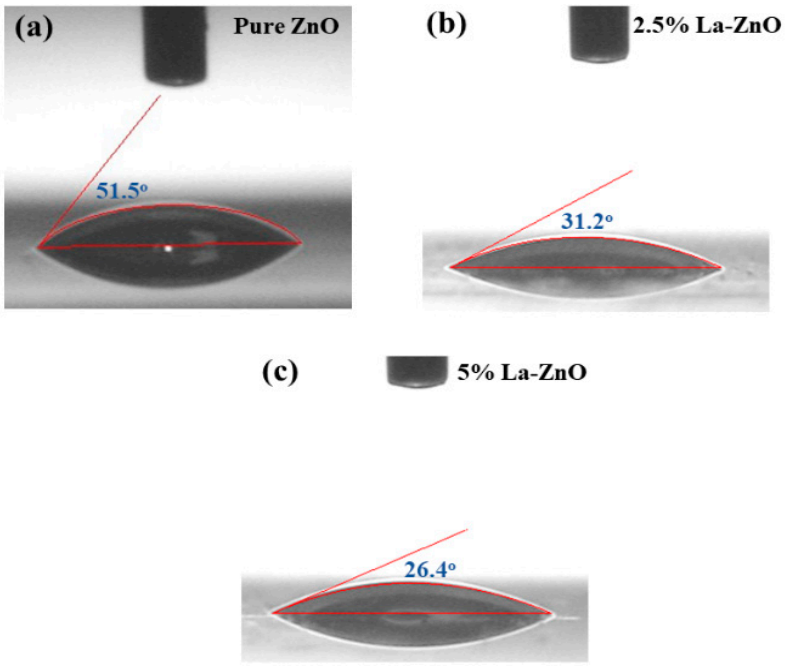

Figure 6. Water Contact Angle under for La wt. percentages. (**a**) WCA for pure ZnO, (**b**) WCA for 2.5 wt. % La-doped ZnO, (**c**) WCA for 5 wt. % La-doped ZnO.

4. Conclusions and Future Recommendations

Pure and La-doped ZnO thin films were synthesized using wet chemistry, and their properties in relation to DSSCs were studied. The XRD analysis showed that the films had a hexagonal wurtzite structure, and the SEM analysis revealed granular and sphere-like shapes. The bandgap energy decreased with increasing La concentrations, and the minimum resistance of the film with a 5 wt. % La content was found to be 3.36×10^1 Ω cm. The increase in carrier concentration due to the presence of La^{3+} cations helped to improve the electrical conductivity. The hydrophilicity of the films increased with increasing La concentrations, indicating an increase in surface free energy due to the suppression of a preferred orientation along a particular axis of the ZnO thin films with La doping. This increased hydrophilicity could enhance dye adsorption in photoanode materials. This study provides important insights into the properties of La-doped ZnO thin films and their potential applications in the field of renewable energy, particularly for the development of nanostructures for photoanode materials to be used in DSSCs devices.

Author Contributions: A.S.: Writing, Experimentation, Characterizations; Z.S.K.: Editing, Critical Review; H.P.: Methodology, Editing; H.M.H.: Critical Review. All authors have read and agreed to the published version of the manuscript.

Funding: This research received no external funding.

Institutional Review Board Statement: Not applicable.

Informed Consent Statement: Not applicable.

Data Availability Statement: Not applicable.

Conflicts of Interest: The authors declare no conflict of interest.

References

1. Nguyen, K.Q. Alternatives to grid extension for rural electrification: Decentralized renewable energy technologies in Vietnam. *Energy Policy* **2007**, *35*, 2579–2589. [CrossRef]
2. Hussain, Z.; Khan, Z.; Ali, A.; Ahmad, N.; Qasim, W.; Shabbir, A. Corrosion Behavior of $MoSi_2$ Coated Hastelloy X Utilized in Iodine -Sulfur Cycle for Hydrogen Production Application. *Solid State Phenom.* **2022**, *336*, 35–41. [CrossRef]
3. Qasim, W.; Khan, Z.; Satti, A.; Ali, A.; Shabbir, A.; Hussain, Z. Electrospinning of Cu Doped TiO_2 Nanofibers and their Potential Application in Photoanode of Dye-Sensitized Solar Cells. *Adv. Sci. Technol.* **2022**, *119*, 27–33.
4. Babar, F.; Mehmood, U.; Asghar, H.; Mehdi, M.H.; Khan, A.U.H.; Khalid, H.; Huda, N.U.; Fatima, Z. Nanostructured photoanode materials and their deposition methods for efficient and economical third generation dye-sensitized solar cells: A comprehensive review. *Renew. Sustain. Energy Rev.* **2020**, *129*, 109919. [CrossRef]
5. Ling, T.; Song, J.-G.; Chen, X.-Y.; Yang, J.; Qiao, S.-Z.; Du, X.-W. Comparison of ZnO and TiO_2 nanowires for photoanode of dye-sensitized solar cells. *J. Alloys Compd.* **2013**, *546*, 307–313. [CrossRef]
6. Kashif, M.; Shabbir, A.; Khan, A.A.; Ali, A. Mathematical modelling of angle dependent polarization raman spectroscopy of molybdenum disulfide before and after adding strain agent. *Inorg. Chem. Commun.* **2022**, *146*, 110075. [CrossRef]
7. Xi, Y.; Wu, W.; Fang, H.; Hu, C. Integrated ZnO nanotube arrays as efficient dye-sensitized solar cells. *J. Alloys Compd.* **2012**, *529*, 163–168. [CrossRef]
8. Nguyen, L.T.; Nguyen, L.T.; Duong, A.T.; Nguyen, B.D.; Hai, N.Q.; Chu, V.H.; Nguyen, T.D.; Bach, L.G. Preparation, characterization and photocatalytic activity of La-doped zinc oxide nanoparticles. *Materials* **2019**, *12*, 1195. [CrossRef] [PubMed]
9. Mrabet, C.; Kamoun, O.; Boukhachem, A.; Amlouk, M.; Manoubi, T. Some physical investigations on hexagonal-shaped nanorods of lanthanum-doped ZnO. *J. Alloys Compd.* **2015**, *648*, 826–837. [CrossRef]
10. Anandan, S.; Vinu, A.; Mori, T.; Gokulakrishnan, N.; Srinivasu, P.; Murugesan, V.; Ariga, K. Photocatalytic degradation of 2, 4, 6-trichlorophenol using lanthanum doped ZnO in aqueous suspension. *Catal. Commun.* **2007**, *8*, 1377–1382. [CrossRef]
11. Ahmad, I.; Jamal, M.A.; Iftikhar, M.; Ahmad, A.; Hussain, S.; Asghar, H.; Saeed, M.; Yousaf, A.B.; Karri, R.R.; Al-kadhi, N.S. Lanthanum-zinc binary oxide nanocomposite with promising heterogeneous catalysis performance for the active conversion of 4-nitrophenol into 4-aminophenol. *Coatings* **2021**, *11*, 537. [CrossRef]
12. Shabbir, A.; Khan, Z.; Ali, A.; Qasim, W.; Ahmad, N.; Hussain, Z.; Pervaiz, H. Diamond-Like Carbon Film Deposited via Electrochemical Route for Antireflection Applications in Photovoltaic. *Key Eng. Mater.* **2022**, *928*, 163–175. [CrossRef]
13. Ashna, R.; Yulizar, Y.; Apriandanu, D. *Strobilanthes crispus* (B.) leaf extract-assisted green synthesis of ZnO-La_2O_3 composite and preliminary study of its photocatalytic activity. In *IOP Conference Series: Materials Science and Engineering*; IOP Publishing: Bristol, UK, 2020; Volume 763, p. 012004.
14. Pankove, J. *Optical Processes in Semiconductors*; Prentice-Hall: Englewood Cliffs, NJ, USA, 1971.
15. Lokesh, K.; Kavitha, G.; Manikandan, E.; Mani, G.K.; Kaviyarasu, K.; Rayappan, J.B.B.; Ladchumananandasivam, R.; Aanand, J.S.; Jayachandran, M.; Maaza, M. Effective ammonia detection using n-ZnO/p-NiO heterostructured nanofibers. *IEEE Sens. J.* **2016**, *16*, 2477–2483. [CrossRef]
16. He, H.-Y.; Huang, J.-F.; Fei, J.; Lu, J. La-doping content effect on the optical and electrical properties of La-doped ZnO thin films. *J. Mater. Sci. Mater. Electron.* **2015**, *26*, 1205–1211. [CrossRef]
17. Nundy, S.; Ghosh, A.; Mallick, T.K. Hydrophilic and superhydrophilic self-cleaning coatings by morphologically varying ZnO microstructures for photovoltaic and glazing applications. *ACS Omega* **2020**, *5*, 1033–1039. [CrossRef] [PubMed]
18. Mrabet, C.; Mahdhi, N.; Boukhachem, A.; Amlouk, M.; Manoubi, T. Effects of surface oxygen vacancies content on wettability of zinc oxide nanorods doped with lanthanum. *J. Alloys Compd.* **2016**, *688*, 122–132. [CrossRef]
19. Wang, L.; Wu, F.; Tian, D.; Li, W.; Fang, L.; Kong, C.; Zhou, M. Effects of Na content on structural and optical properties of Na-doped ZnO thin films prepared by sol–gel method. *J. Alloys Compd.* **2015**, *623*, 367–373. [CrossRef]
20. Shaban, M.; El Sayed, A. Effects of lanthanum and sodium on the structural, optical and hydrophilic properties of sol–gel derived ZnO films: A comparative study. *Mater. Sci. Semicond. Process.* **2016**, *41*, 323–334. [CrossRef]